DOI 10.1007/s11182-020-02011-9

Russian Physics Journal, Vol. 63, No. 1, May, 2020 (Russian Original No. 1, January, 2020)

EFFECT OF HIGH TEMPERATURE AND HIGH STRESS-ASSISTED AUSTENITE AGING ON MARTENSITIC TRANSFORMATIONS IN HIGH-STRENGTH Ti – 51.8 ат.% Ni SINGLE CRYSTALS

E. E. Timofeeva,[1] E. Yu. Panchenko,[1] A. I. Tagiltsev,[1] Yu. I. Chumlyakov,[1] M. V. Zherdeva,[1] and V. A. Andreev[2,3]

UDC 669.24.1.871–539.371:548.55

High-strength materials containing dispersed Ti_3Ni_4 *particles (d ~ 800 nm) and exhibiting superelasticity (SE) in a wide temperature range from 200 to 450 K were designed by aging at 823 K, 1 h of nickel-rich [001]-oriented* Ti–*51.8 at.%* Ni *single crystals. The influence of the stress-assisted austenite aging in different regimes (temperature, applied stress, and time) on the stability of the shape memory effect (SME) and SE is studied. It is shown that the single crystals are stable to stress-assisted austenite aging in the entire SE temperature range at T < 523 K under a stress of* $0.8\sigma_{cr}$*. An increase in the temperature to 523–573 K for stress-assisted (1400 MPa) and stress-free aging time 1–10 h leads to precipitation of nanosized* Ti_3Ni_4 *particles and changes the SE and SME evolution. The largest effect of increase in the* M_s *temperature by 22–27 K during SME, decrease in the critical stress* σ_{cr} *during SE (by 10–34%), and increase in the deformation hardening coefficient* $\theta = d\sigma/d\varepsilon$ *and the coefficient of critical stress growth with temperature* $\alpha = d\sigma/dT$ *was observed after aging at 573 K for 10 h (0 and 1400 MPa).*

Keywords: martensitic transformations, shape memory effect, superelasticity, hysteresis, aging, single crystals.

INTRODUCTION

Titanium nickelide is a widely investigated alloy with shape memory effect (SME) that finds variety of applications from medicine to space industry [1−3] due to large reversible strain, corrosion resistance, etc. To use the Ti−Ni alloys under high stresses and temperatures (exceeding 373 K), a high strength alloy is required. For this purpose, alloys with high content of nickel (exceeding 51.2 at.%) are used [1, 3, 4]. However, the rise of nickel concentration not only increases the alloy strength, but also decreases temperatures of *B*2–*B*19′ martensitic transformations (MT) [1, 3, 5, 6]. Therefore, quenched single-phase high-nickel alloys are subject to aging that leads to precipitation of Ti_3Ni_4 particles [1, 3]. The particles reduce the matrix supersaturation with nickel, increase the MT temperatures, change the twinning type into the compound one, and increase the strength properties (depending on the size of particles) [7, 8]. The yield strength level of the *B*2 phase can be additionally increased and the high-temperature superelasticity (SE) can be obtained by choosing single crystals with [001]-orientation for which the Schmid factor for *a* <100> {011} and *a* <001> {001} slip systems in the *B*2 phase is zero [3, 5, 9−11].

However, the exploitation of the material at high temperatures under stress intensifies the diffusion processes [12, 13] and can change the functional properties even of high-strength alloys. Namely, stress-assisted aging at high

[1]V. D. Kuznetsov Siberian Physical-Technical Institute at Tomsk State University, Tomsk, Russia, e-mail: katie@sibmail.com; panchenko@mail.tsu.ru; antontgl@gmail.com; chum@phys.tsu.ru; zhmv98@mail.ru; [2]"MATEKS-SPF" Industrial Center, Moscow, Russia, e-mail: andreev.icmateks@gmail.com; [3]A. A. Baikov Institute of Metallurgy and Materials Science of the Russian Academy of Sciences, Moscow, Russia. Translated from Izvestiya Vysshikh Uchebnykh Zavedenii, Fizika, No. 1, pp. 114–120, January, 2020. Original article submitted November 5, 2019.

 1064-8887/20/6301-0126 ©2020 Springer Science+Business Media, LLC

temperature can lead to the relaxation processes, relief of internal stresses, redistribution of point defects in accordance with the symmetry of the crystal lattice, and precipitation of secondary phase particles [1, 3, 6, 14]. As a consequence, the special features of MT change together with the MT temperatures, thermal and stress hysteresis, level of critical stresses, and so on. To control these properties, the kinetics of the SME and SE must be investigated after stress-assisted austenite aging at high temperatures.

According to the above-stated, an urgent problem is the design of high-strength alloys with highly stable functional properties. Therefore, this work is aimed at the design of high-strength nickel-rich [001]-oriented Ti–Ni (C_{Ni} > 51.2 at.%) single crystals with wide SE interval and the study of the SME and SE stabilities to stress-assisted austenite aging depending on the temperature, aging time, and applied stress.

1. EXPERIMENTAL TECHNIQUE

The Ti–Ni single crystals were grown by the Bridgeman method. The samples for compression tests were shaped as parallelepipeds with sizes of 3 × 3 × 6 mm. The MT temperatures were determined from the temperature dependence of the electrical resistance. The mechanical tests and aging were carried out using an electromechanical machine Instron VHS 5969 and an IMRS-1 dilatometer. The error of temperature measurement was ±2 K, and the error of strain measurement was ±0.3%. Electron microscopic studies were carried out by using a JEOL JEM-2100 microscope (the Nanotekh Shared Use Center of the ISPMS SB RAS).

The high strength of the examined Ti–Ni alloy is provided by the choice of:

– chemical composition of the nickel-rich Ti – 51.8 at.% Ni alloy,

– thermal treatment including high-temperature annealing at 1253 K, 1 h, followed by water quenching, and subsequent aging at 823 K, 2.5 h with water quenching,

– high strength [001]-orientation [3, 5, 9].

The stress-free or stress-assisted austenite aging was performed under stresses that did not exceed 80% of the critical stress σ_{cr} of the MT onset at temperatures of 348–573 K. Such stresses allowed exploitation conditions to be modeled and the onset of plastic strain to be avoided. The aging time was 1–10 h. After aging, no irreversible strain was observed in all samples.

First, to study the influence of aging on the stress-assisted MT, the SME was investigated in stress-assisted cooling/heating cycles to obtain the curves $\varepsilon(T)$. A stress of 300 MPa was used to reach the maximum reversible strain and to avoid the irreversible strain. The temperature M_s^σ of the start of stress-assisted MT upon cooling, the interval Δ_1^σ of the forward stress-assisted MT, and the magnitude of thermal hysteresis ΔT_σ were determined from the curves $\varepsilon(T)$. Second, the SE was investigated in loading/unloading cycles at different temperatures to obtain the curves $\sigma(\varepsilon)$ from which the critical stress σ_{cr}, the strain hardening coefficient $\theta = d\sigma/d\varepsilon$, and the coefficient of growth of the critical stress σ_{cr} with temperature $\alpha = d\sigma_{cr}/dT$ were determined.

2. RESULTS OF EXPERIMENT AND DISCUSSION

It was experimentally shown (Fig. 1) that aging at 823 K, 2.5 h led to precipitation of large lenticular Ti_3Ni_4 particles with $\{111\}_{B2}$-type habitus plane. Areas with different particle morphology were observed: 1) multivariate arrangement of particles with $d \sim 800$ ns (Fig. 1*a*) and 2) prevalence of oriented particles (particles approach each other forming ensembles of wavy parallel plates 1–3 μm long, Fig. 1*b*). Similar particle morphology was observed in [15] for Ti–Ni polycrystals at close aging temperatures.

Upon stress-free cooling/heating, single crystals undergo the forward *B*2–*R*–*B*19′ and the reverse *B*19′–*R*–*B*2 MT (Fig. 2*a*). This is in agreement with [1, 3, 5, 11]. The MT temperatures determined from the temperature dependence of the electrical resistance were T_R = 265 K, M_s = 183 K, M_f = 149 K, A_s = 199 K, and A_f = 221 K.

Figure 2*b* shows the temperature dependence of the critical stress of martensite formation for initial aged Ti – 51.8 at.% Ni single crystals. The dependence was obtained from the curves $\sigma(\varepsilon)$ recorded in loading/unloading cycles.

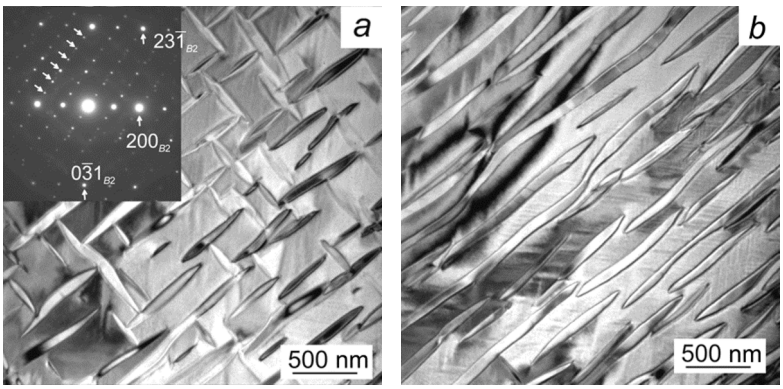

Fig. 1. Microstructure of initial aged Ti – 51.8 at.% Ni crystals: bright-field images and corresponding selected electron area diffraction pattern with the $[013]_{B2}$ zone axis; the arrows indicate reflections from Ti_3Ni_4 particles.

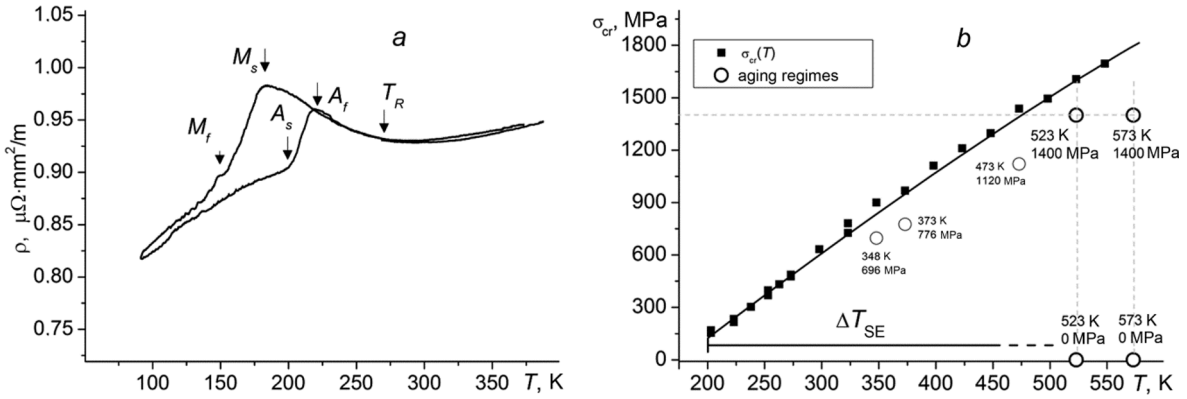

Fig. 2. Temperature dependences of the electrical resistance (*a*) and of the critical stress of martensite formation (*b*) for initial [001]-oriented Ti – 51.8 at.% Ni crystals.

The stress σ_{cr} increased with temperature in accordance with the Clapeyron–Clausius equation [1, 3]. As can be seen from the figure, the high-strength state with a wide interval of SE was formed in single crystals because of aging. The strain (up to 3.5%) in loading/unloading cycles in the range from 200 K to 450 K was completely reversible process. At temperatures above 450 K, the SE was also observed; however, the fragile destruction of samples occurred when the reversible strain in the cycle exceeded 2.0%. Thus, the interval of SE exceeded 250 K and was one of the widest among Ti–Ni alloys [1, 3, 5, 11].

Figure 2*b* illustrates the aging regimes. It was experimentally established that the stress-assisted aging at temperatures higher than 523 K does not affect the stress-assisted MT, SME, and SE. In the subsequent thermal stress-assisted cooling/heating cycles, the temperature M_s^{σ} and the thermal hysteresis ΔT did not change the same as the parameters of the SE curves in loading/unloading cycles. Hence, the choice of the chemical composition, the thermal treatment, and the orientation allowed the high-strength Ti–Ni single crystals with high thermomechanical SE stability to be formed in the entire interval of SE observation. However, aging at 523 K and higher temperatures influences on the stress-assisted MT (Fig. 3). Hence, overheating above 523 K during exploitation can change the functional properties. For more detailed study, stress-free (0 MPa) and stress-assisted (1400 MPa) aging were carried out at 523 and 573 K.

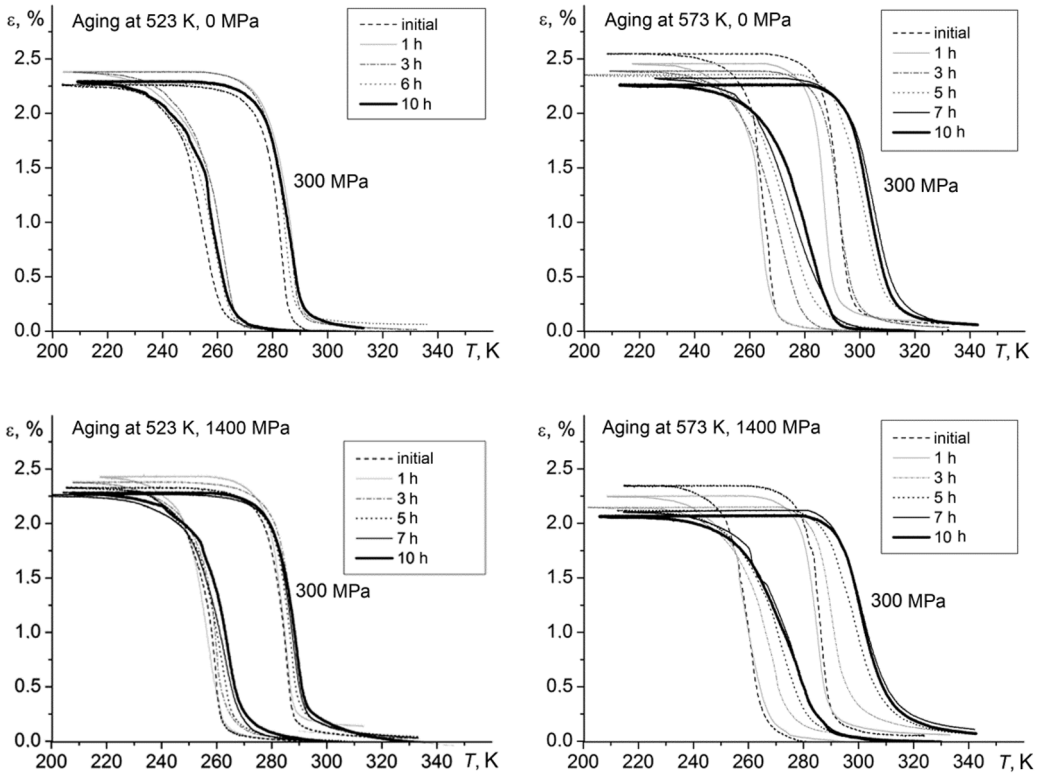

Fig. 3. ε(*T*) response during the SME (in cooling/heating cycles under compressive stress of 300 MPa) in initial [001]-oriented Ti – 51.8 at.% Ni single crystals and after aging at 523 and 573 K (0 and 1400 MPa), 1–10 h.

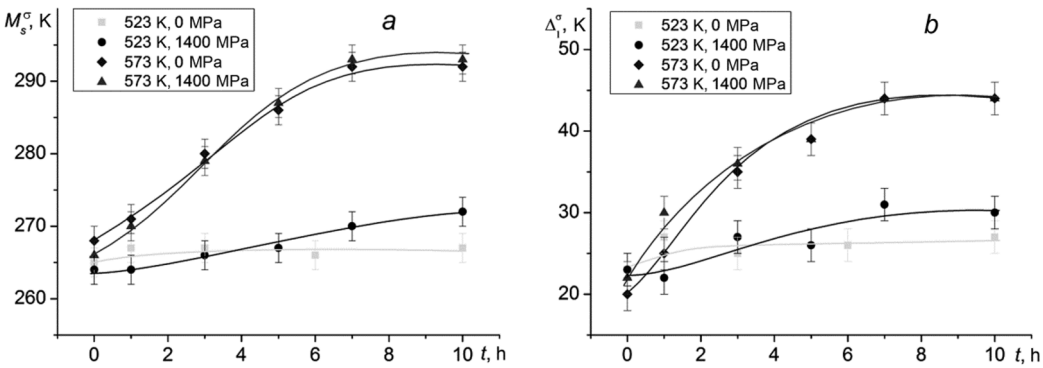

Fig. 4. Kinetics of M_s^σ temperature changes (*a*) and interval Δ_1^σ (*b*) depending on the aging regime for aged [001]-oriented Ti – 51.8 at.% Ni single crystals.

After aging at 523 K, 10 h, 0 MPa, the changes in the temperature M_s^σ and in the interval Δ_1^σ were minimal and compared to those in the initial state; they did not exceed the error values (Figs. 3 and 4). However, the application of a high stress of 1400 MPa during aging at 523 K, 10 h led to a small increase in the temperature M_s^σ and Δ_1^σ by

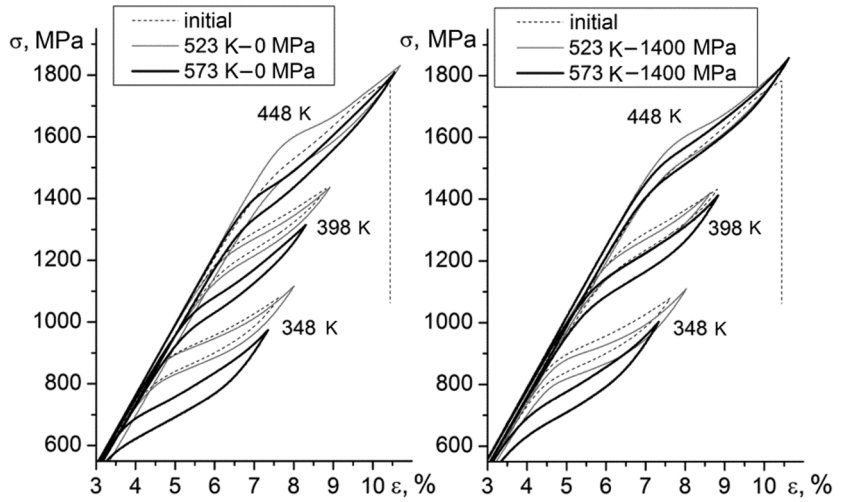

Fig. 5. σ(ε) response during SE (at 348, 373, and 398 K) in initial [001]-oriented Ti – 51.8 at.% Ni single crystals and after aging at 523 and 573 K (0 and 1400 MPa), 10 h.

8 K. The thermal hysteresis ΔT_{σ} and the reversible strain remained unchanged after aging at 523 K, and the SME magnitude was $\varepsilon_{tr} = (2.3 \pm 0.3)\%$ (Figs. 3 and 4).

An increase in the stress-free and stress-assisted (1400 MPa) aging temperature to 573 K, 10 h caused the increase of the temperature M_s^{σ} and interval Δ_1^{σ} by 22 and 27 K, respectively (Figs. 3 and 4). The SME strain after 10 h aging at 573 K (0 and 1400 MPa) decreased by 0.3%. The thermal hysteresis did not change after stress- free aging at 573 K, 10 h and increased from 25 to 31 K after stress-assisted (1400 MPa) aging at 573 K, 10 h. Thus, the SME parameters were significantly influenced by the increase of the aging temperature (from 523 to 573 K) compared to the influence of the applied stress (0 or 1400 MPa).

Figure 5 shows the results of SE investigation at the indicated test temperatures close to 373 K in single crystals before and after aging at 523 and 573 K. The SE loops were obtained after maximal aging time of 10 h. As can be seen from Fig. 5, the aging at 523 K, 0–1400 MPa practically did not influence on the behavior of the curves σ(ε): the critical stress σ_{cr} and the strain hardening coefficient $\theta = d\sigma/d\varepsilon$ change slightly. The aging at 573 K caused a decrease in the critical stress σ_{cr}, which is explained as follows. The increase in M_s^{σ} shifts the dependence $\sigma_{cr}(T)$ toward higher temperatures. Hence, at the same fixed test temperature, the value of the critical stress will be lower in samples with higher temperature M_s^{σ}. After aging at 573 K (0 and 1400 MPa), a maximum decrease of σ_{cr} is observed compared to the initial state. At test temperature of 348 K, the critical stress decreased by 32–34%, whereas at a higher test temperature of 398 K, it decreased only by 10–14%. This means that after aging, the coefficient of growth of critical stress σ_{cr} with temperature $\alpha = d\sigma_{cr}/dT = 8.1$ MPa/K increases compared to initial crystals in which $\alpha = d\sigma_{cr}/dT = 6.5$ MPa/K.

After aging, the strain hardening coefficient $\theta = d\sigma/d\varepsilon$ also increased. Whereas $\theta = d\sigma/d\varepsilon$ in the initial crystals was $62 \cdot 10^2$ MPa, after aging at 573 K, 10 h, $\theta = d\sigma/d\varepsilon$ increased to $76 \cdot 10^2$ MPa. All the above-described changes testify to the precipitation of particles of secondary phase during aging. As follows from [16], aging of Ti–Ni alloys (C_{Ni} = 50.6–50.9 at.%) at 523–573 K allows Ti_3Ni_4 particles with sizes $d < 10$ nm to be obtained.

Indeed, electron microscopic studies after aging at 573 K, 5 h, 1400 MPa show (Fig. 6) that nanosized particles are additionally precipitated between large Ti_3Ni_4 particles comprised in initial aged single crystals. It is important to note that the nanosized particles are also precipitated along the particle-matrix interfaces framing large particles. This was also observed in [17, 18]. Since the $[001]_{B2}$ axis of stress application during aging is equivalently arranged with

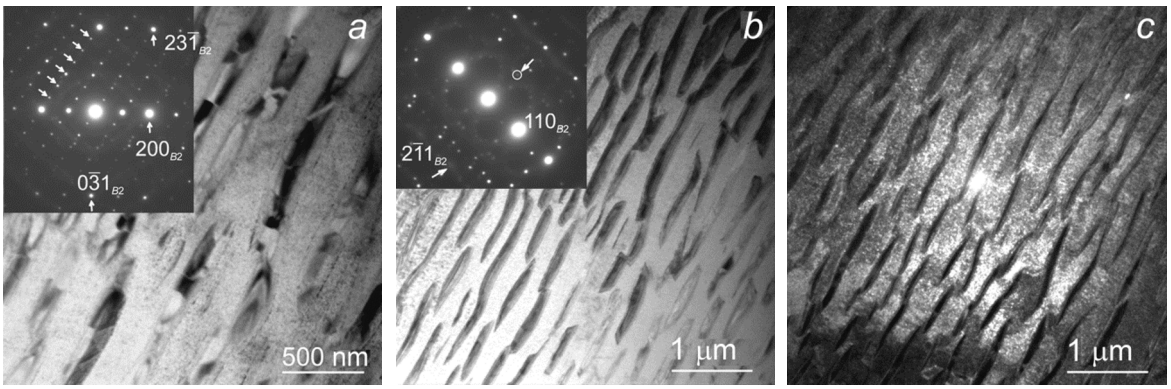

Fig. 6. Microstructure of aged Ti – 51.8 at.% Ni crystals after aging at 573 K, 5 h, 1400 MPa: bright field image showing large and small Ti_3Ni_4 particles (*a*); bright field image and selected electron area diffraction pattern with the zone axis close to $[\bar{1}13]_{B2}$ (*b*); and dark field image in the circled reflection that shows small Ti_3Ni_4 particles (*c*).

respect to all axes of the $\{111\}_{B2}$ type along which the normals of the particle habit planes are oriented, particle variants are not selected during aging, and the four variants are observed as during stress-free aging.

First, precipitation of Ti_3Ni_4 particles decreases the nickel content in the matrix that according to [1, 3, 5, 6], increases the MT temperatures. Second, particles do not undergo the MT and decrease the volume fraction of the *B*2 matrix that undergoes the transition. This slightly reduces the reversible strain ε_{tr} and, according to the Clapeyron–Clausius equation, increases the coefficient $\alpha = d\sigma_{cr}/dT \sim 1/\varepsilon_{tr}$ observed after aging at 573 K (Figs. 3 and 5). Third, the nanosized Ti_3Ni_4 particles cause hardening of the *B*2 matrix and *B*19' martensite.

As can be seen from Fig. 4, an increase in the aging time to more than 5 h weakly influences on the temperature M_s^σ, SME, and SE. By this time, a considerable volume fraction of nanosized particles has already been precipitated, thereby decreasing the nickel content and strengthening the *B*2 phase and increasing the stability of the alloy to further aging. Hence, we can conclude that the formation of the microstructure with a bimodal size distribution of Ti_3Ni_4 particles is an effective method of improving the mechanical and functional characteristics.

Fourth, according to [3, 7, 8], the precipitation of nanosized particles increases the density of the compound $(001)_{B19'}$ twins, that is, the surface energy ΔG_{surf} increases. During the stress-assisted MT, the nanosized particles are elastically deformed and accumulate the elastic energy ΔG_{el}. Hence, the reversible component of non-chemical stress-free energy $\Delta G_{rev} = \Delta G_{el} + \Delta G_{surf}$ increases. Table 1 presents values of the ratio of reversible to irreversible energy [3, 19]:

$$\Delta G_{rev}/2\Delta G_{irr} = (\Delta_1^\sigma + \Delta_2^\sigma)/2\Delta T_\sigma. \quad (1)$$

The values of the ratio $\Delta G_{rev}/2\Delta G_{irr}$ were obtained from the curves $\varepsilon(T)$ after aging at 523 and 573 K (0 and 1400 MPa), 10 h (Fig. 3). In the initial aged crystals upon cooling under compressive stress of 300 MPa, the MT of the first type according to the Tong–Weiman classification is observed characterized by $A_s > M_s$, $\Delta G_{rev}/2\Delta G_{irr}$ not exceeding 1, and large energy dispersion during the MT. The MT type remains unchanged after aging at 523 K, 10 h, 0 and 1400 MPa, that weakly influences the functional properties of the single crystals (see Table 1). However, aging at 573 K, 10 h, 0 and 1400 MPa changed the MT type to the second one with considerable accumulation of the reversible energy during the forward MT. This is caused by the precipitation of nanosized particles when the ratio $\Delta G_{rev}/2\Delta G_{irr}$ becomes greater than 1 and $A_s < M_s$. Since the temperature interval Δ_1^σ is proportional to the reversible energy ΔG_{rev}, an increase in ΔG_{rev} caused the interval Δ_1^σ to increase. Such change of the MT type after precipitation of nanosized particles was observed in Ti–Ni alloys and other materials with a shape memory effect [2].

TABLE 1. Ratios $\Delta G_{rev}/2\Delta G_{irr}$ for the Initial Aged Single Crystals and after Aging (Calculated from the Curves $\varepsilon(T)$ Shown in Fig. 3)

State	Aging regime			
	523 K		573 K	
	0 MPa	1400 MPa	0 MPa	1400 MPa
Initial	0.82	0.85	0.70	0.87
Aging for 10 h	0.96	1.04	1.74	1.46

CONCLUSIONS

It has been established experimentally that the heterophase [001]-oriented Ti – 51.8 at.% Ni single crystals comprising large disperse Ti_3Ni_4 particles ($d \sim 800$ nm) form the unique high-strength single crystals after thermal treatment at 1253 K, 1 h + 823 K, 2.5 h in which the SE is observed at temperatures from 200 to 450 K. The following special features of the influence of the stress-assistant austenite aging on the functional properties of the heterophase [001]-oriented Ti – 51.8 at.% Ni single crystals were established:

1. Aging at temperatures up to 523 K under stresses of $0.8\sigma_{cr}$ do not influence on the pattern of the stress-assisted *B*2–*R*–*B*19' MT evolution, SME, and SE.

2. Stress-free aging at temperatures of 523–573 K, 1400 МПа, 1–10 h and aging under stress of 1400 MPa cause the recipitation of nanosized Ti_3Ni_4 particles and change the patterns of SE and SME defined by the aging regime (temperature and applied stress).

3. Aging at 573 K, 10 h (0 or 1400 MPa) increases the M_s^{σ} temperature by 22–27 K during SME, reduces the critical stress σ_{cr} during SE (by 32–34% at 323 K and by 10–14% at 398 K), and increases the strain hardening coefficient $\theta = d\sigma/d\varepsilon$ and the coefficient of growth of critical stress σ_{cr} with temperature $\alpha = d\sigma_{cr}/dT$ by a factor of 1.2.

4. It is possible to increase the thermomechanical stability of the heterophase [001]-oriented Ti – 51. 8 at.% Ni single crystals comprising large Ti_3Ni_4 particles by additional low-temperature aging providing precipitation of nanosized Ti_3Ni_4 particles.

This work was supported in part by the Russian Science Foundation (grant No. 18-19-00298).

REFERENCES

1. K. Otsuka, Shape Memory Materials, Cambridge University Press, Cambridge (1998).
2. J. Mohd Jani, M. Leary, A. Subic, and M. A. Gibson, Mater. Des., **56**, 1078–1113 (2014).
3. Y. I. Chumlyakov, I. V. Kireeva, E. Y. Panchenko, *et al*., in: Shape Memory Alloys: Properties, Technologies, Opportunities, Trans Tech Publications Ltd, Switzerland (2015), pp. 108–174.
4. H. Sehitoglu, J. Jun, X. Zhang, *et al*., Acta Mater., **49**, 3609–3620 (2001).
5. I. Kaya, H. E. Karaca, M. Souri, *et al*., Mater. Sci. Eng. A, **686**, 73–81 (2017).
6. K. Otsuka and X. Ren, Scripta Mater., **50**, 207–212 (2004).
7. T. Waitz, T. Antretter, F. D. Fischer, *et al*., J. Mech. Phys. Solids, **55**, 419–444 (2007).
8. T. Waitz, Acta Mater., **53**, 2273–2283 (2005).
9. E. Acar, H. E. Karaca, B. Basaran, *et al*., Mater. Sci. Eng. A, **573**, 161–165 (2013).
10. E. E. Timofeeva, N. Yu. Surikov, A. I. Tagiltsev, *et al*., J. Alloys Compd., **817**, 152719 (2019).
11. E. E. Timofeeva, E. Yu. Panchenko, YU. I. Chumlyakov, et al., Russ. Phys. J., **61**, No. 5, 821–827 (2018).
12. D. L. Olmsted, R. Phillips, and W. A. Curtin, Mater. Sci. Eng., **12**, 781–797 (2004).
13. M. J. Aziz, Appl. Phys. Lett., **70**, No. 21, 2810–2812 (1997).
14. S. Kustov, J. Pons, E. Cesari, and J. Van Humbeeck, Acta Mater., **52**, 4547–4559 (2004).

15. V. G. Pushin, V. V. Kondrat'ev, and V. N. Khachin, Pretransitive Phenomena and Martensitic Transformations, Publishing House of the Ural Branch of the Russian Academy of Sciences, Ekaterinburg (1998).
16. J. I. Kim and S. Miyazaki, Acta Mater., **53**, 4545–4554 (2005).
17. R. Ducher, R. Kainuma, and K. Ishida, J. Alloys Compd., **463**, 213–219 (2008).
18. E. Dogan, I. Karaman, Y. I. Chumlyakov, and Z. P. Luo, Acta Mater., **59**, 1168–1183 (2011).
19. P. Wollants, J. R. Roos, and L. Delaey, Prog. Mater. Sci., **37**, 227–288 (1993).